

12-29-1994

## Transmission Electron Microscopy, High Resolution X-Ray Diffraction and Rutherford Backscattering Study of Strain Release in InGaAs/GaAs Buffer Layers

G. Salviati  
*C.N.R. MASPEC Institute*

L. Lazzarini  
*C.N.R. MASPEC Institute*

C. Ferrari  
*C.N.R. MASPEC Institute*

P. Franzosi  
*C.N.R. MASPEC Institute*

S. Milita  
*C.N.R. MASPEC Institute*

Follow this and additional works at: <https://digitalcommons.usu.edu/microscopy>

 Part of the [Biology Commons](#)  
See next page for additional authors

### Recommended Citation

Salviati, G.; Lazzarini, L.; Ferrari, C.; Franzosi, P.; Milita, S.; Romanato, F.; Berti, M.; Mazzer, M.; Drigo, A. V.; Bruni, M. R.; Simeone, M. G.; and Gambacorti, N. (1994) "Transmission Electron Microscopy, High Resolution X-Ray Diffraction and Rutherford Backscattering Study of Strain Release in InGaAs/GaAs Buffer Layers," *Scanning Microscopy*. Vol. 8 : No. 4 , Article 21.

Available at: <https://digitalcommons.usu.edu/microscopy/vol8/iss4/21>

This Article is brought to you for free and open access by the Western Dairy Center at DigitalCommons@USU. It has been accepted for inclusion in Scanning Microscopy by an authorized administrator of DigitalCommons@USU. For more information, please contact [digitalcommons@usu.edu](mailto:digitalcommons@usu.edu).

---

# Transmission Electron Microscopy, High Resolution X-Ray Diffraction and Rutherford Backscattering Study of Strain Release in InGaAs/GaAs Buffer Layers

## Authors

G. Salviati, L. Lazzarini, C. Ferrari, P. Franzosi, S. Milita, F. Romanato, M. Berti, M. Mazzer, A. V. Drigo, M. R. Bruni, M. G. Simeone, and N. Gambacorti

## TRANSMISSION ELECTRON MICROSCOPY, HIGH RESOLUTION X-RAY DIFFRACTION AND RUTHERFORD BACKSCATTERING STUDY OF STRAIN RELEASE IN InGaAs/GaAs BUFFER LAYERS

G. Salviati<sup>1,\*</sup>, L. Lazzarini<sup>1</sup>, C. Ferrari<sup>1</sup>, P. Franzosi<sup>1</sup>, S. Milita<sup>1</sup>, F. Romanato<sup>2</sup>,  
M. Berti<sup>2</sup>, M. Mazzer<sup>2</sup>, A.V. Drigo<sup>2</sup>, M.R. Bruni<sup>3</sup>, M.G. Simeone<sup>3</sup> and N. Gambacorti<sup>3</sup>

<sup>1</sup>C.N.R.- MASPEC Institute, Via Chiavari 18/A, I-43100 Parma, Italy

<sup>2</sup>University of Padova, Physics Department, Via Marzolo 8, I-35131 Padova, Italy

<sup>3</sup>C.N.R.- ICMAT Institute, Via Salaria Km 29 Monterotondo, I-00015 Roma, Italy

(Received for publication May 7, 1994 and in revised form December 29, 1994)

### Abstract

Strain release and dislocation distribution in InGaAs/GaAs double heterostructures, step-graded and linear-graded buffer layers have been studied. A higher misfit dislocation density at the inner interface between the InGaAs layer and the substrate was found in all the samples. This corresponded to a strain release of the inner ternary layers much larger than predicted by equilibrium theories. The residual parallel strain of the external layers as a function of their thickness was found to follow a curve approximately of slope -0.5, in agreement with previous investigations on single InGaAs layers. This result has been interpreted as evidence that the elastic energy per unit interface area remains constant during the epilayer growth. The presence of numerous single and multiple dislocation loops inside the substrate was attributed to the strain relaxation occurring through dislocation multiplication via Frank-Read sources activated during the growth. A comparison with InGaAs/GaAs step-graded and linear-graded heterostructures is also shown and briefly discussed.

Finally, lattice plane tilts between epilayers and substrates have been found due to the imbalance in the linear density of misfit dislocations with opposite component of the Burgers vector,  $b \perp^{\text{eff}}$ , perpendicular to the interface.

**Key Words:** Misfit dislocations, threading dislocations, strain release, dislocation loops, lattice plane tilts.

\*Address for correspondence:

Giancarlo Salviati  
CNR-MASPEC Institute,  
via Chiavari 18/A,  
43100 Parma,  
Italy

Telephone number: +39 521 269223  
FAX number: +39 521 269206

### Introduction

The study of plastic relaxation and nucleation of extended defects in lattice mismatched heterostructures is important in view, for instance, of integrated optoelectronics that demand the ability of growing buffer layers in which plastic relaxation provides the change in the lattice constant. A good buffer layer should be fully relaxed and should prevent the propagation of threading dislocations into the active layers of the devices. In the last couple of years, several groups have revisited the old idea of growing linearly or step-graded buffer layers between the substrate and the epilayer in order to reduce the dislocation density in the active layer, both in SiGe/Si and InGaAs/GaAs heterostructures [2, 4, 9, 10, 15, 17, 19, 20, 21].

In order to study the confinement of the dislocations in the buffer-substrate interface and the mechanism of strain release in multiple structures, following our previous work on InGaAs/GaAs single and superlattice buffer layers [6, 25], a set of molecular beam epitaxy (MBE) grown  $\text{In}_x\text{Ga}_{1-x}\text{As}/\text{GaAs}$  double heterostructures, of nominal In content  $x_1 = 0.05$  and  $x_2 = 0.10$  and total nominal thickness  $t = 500$  nm have been studied. Three additional specimens of identical compositions and nominal thickness of the inner layer  $t_1 = \text{constant} = 120$  nm and of the external one  $80 < t_2 < 185$  nm were also grown for studying the dislocation propagation during the upper layer growth with respect to the total strain content in the structures. Further, compositionally step-graded and linear-graded heterostructures with nominal composition  $0.10 < x < 0.30$  and thickness  $t_{\text{sg}} = 1.42$   $\mu\text{m}$  and  $t_{\text{lg}} = 1.02$   $\mu\text{m}$  respectively were also studied.

### Experimental

The structures, sketched in Figure 1, have been grown at Istituto di Chimica dei Materiali (ICMAT) in a conventional MBE system on Si doped GaAs substrates with an average dislocation density of  $5.5 \times 10^2$   $\text{cm}^{-2}$  and on semi-insulating GaAs single crystals with a dislocation density of about  $5 \times 10^4$   $\text{cm}^{-2}$ . All the

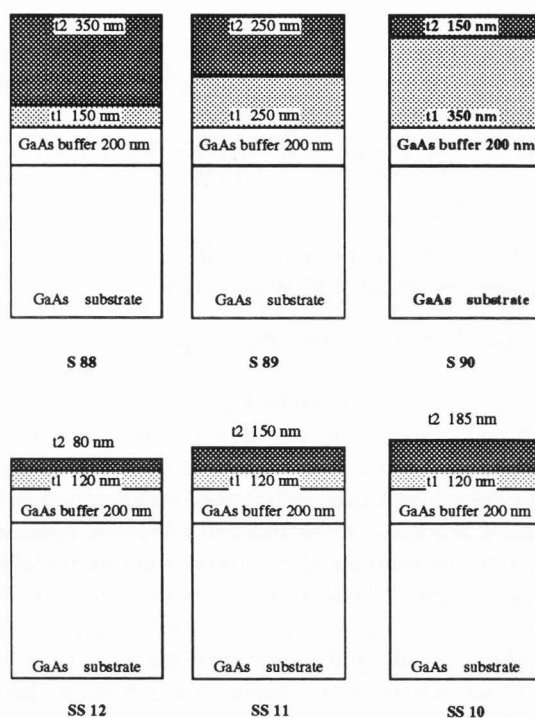


**Figure 1.** Sketch of the  $\text{In}_x\text{Ga}_{1-x}\text{As}/\text{GaAs}$  double heterostructures investigated. The nominal In content are  $x(t_2) = 0.10$ , and  $x(t_1) = 0.05$ .

substrates were nominally (001) oriented within  $0.5^\circ$ . A standard wet etching procedure was used for substrate preparation in order to obtain a thin oxide film as passivation layer. Before the growth, this was removed by heating at  $580\text{--}600^\circ\text{C}$  under arsenic flux. The substrate temperature was kept constant at  $530^\circ\text{C}$  for all the samples. The buffer and ternary growth rates were determined by reflection high energy electron diffraction (RHEED) oscillations. Consequently, the In content in the alloy was also determined. In order to keep the In and Ga fluxes, and therefore the In concentration in the alloy, constant, the  $\text{In}_{0.05}\text{Ga}_{0.95}\text{As}$  layer was grown first. After the growth of the first layer, each sample was left in the buffer chamber in high vacuum conditions ( $P \approx 5 \cdot 10^{-9}$  Torr). Subsequently, the  $\text{In}_{0.1}\text{Ga}_{0.9}\text{As}$  layer was grown on each sample varying the In flux conditions to obtain the exact In concentration. The V/III pressure ratio was kept around 27-35.

All the specimens have been studied by comparing transmission electron microscopy (TEM), high resolution X-ray diffraction (HRXRD) and Rutherford backscattering (RBS) and channeling investigations. RBS and HRXRD techniques have been employed for measuring the composition, the thickness, and the degree of strain release of the samples. (110) oriented cross-sectional TEM (XTEM) and (001) oriented plan view investiga-

tions were carried out for studying the dislocation nature, distribution and density inside the structures. Room temperature panchromatic cathodoluminescence (PCL) in the scanning electron microscope (SEM) and  $\text{CrO}_3\text{-H}_2\text{O-HF}$  diluted Sirtl-like solution with light activation (DSL) were also employed for large area investigations of the misfit dislocation planar distribution and of the threading dislocations density. RBS channeling measurements were carried out at the Laboratori Nazionali di Legnaro by using a high precision goniometer sample holder and  $^4\text{He}^+$  beam of 2 MeV energy [7].

TEM analyses were performed at MASPEC in a JEOL 2000FX microscope operating at an accelerating voltage of 200 kV on samples mechano-chemically thinned and then finished by room temperature Ar ion milling. SEM-PCL studies were also carried out at MASPEC in a 250 MK2 Cambridge Stereoscan, both in the emission and transmission geometries at accelerating voltages ranging between 7 and 20 kV.

X-ray measurements were performed at MASPEC on a double crystal diffractometer in the  $117 \text{ CuK}\alpha$  parallel geometry, corresponding to a Bragg angle  $\theta_B$  of  $76.64^\circ$  and an asymmetry angle  $\phi = \pm 11.4^\circ$  or  $335^\circ$  parallel geometry with  $\theta_B = 63.3^\circ$  and  $\phi = \pm 40.32^\circ$ .

The 117 reflection gave a large peak splitting, thus permitting better separation of the layer peaks in the diffraction profile. In order to obtain the lattice mismatches parallel,  $(\Delta d/d)^\parallel$ , and perpendicular,  $(\Delta d/d)^\perp$ , to the (100) surface, the measurements were performed both in the grazing incidence (positive  $\phi$ ) and the grazing emergence (negative  $\phi$ ) geometry. For each geometry, four independent measurements were repeated after successive  $90^\circ$  rotations around the surface normal. To avoid the effect of small deviations of the surface from the nominal (100) crystallographic plane and to measure the tilt of the layer lattice with respect to the substrate, the measurements were repeated after  $180^\circ$  rotations along the surface normal. In this way, two independent measurements of the lattice tilts and  $\Delta d/d$  in the scattering planes corresponding to the  $0^\circ\text{--}180^\circ$  and  $90^\circ\text{--}270^\circ$  rotations were obtained. The mismatch values  $\Delta d/d$  have been calculated from the measured values of the peak splitting,  $\Delta_{\text{Tot}}$ , using the exact formula:

$$\Delta_{\text{Tot}} = \Delta\phi + \Delta\theta_B = \phi - t_g^{-1} [t_g\phi \{(1 + (\Delta d/d)^\perp)\} / \{1 + (\Delta d/d)^\parallel\}] + \sin^{-1} [\sin\theta_B \{\sin^2\phi(1 + (\Delta d/d)^\perp)^2 + \cos^2\phi(1 + (\Delta d/d)^\perp)^2\}]^{1/2} - \theta_B \quad (1)$$

where  $\Delta\phi$  is the tilt of the lattice planes due to the deformation of the layer lattice and  $\Delta\theta_B$  is the change of the Bragg angle.

**Table 1.** Experimental values of composition,  $x$ ; thickness,  $t$ ; and residual strain,  $\epsilon_{\text{res}}$ , of the specimens investigated. The average error values are also reported.

Sample	$x(t_1)$ % ( $\pm 0.3$ %)	$x(t_2)$ % ( $\pm 0.3$ %)	$t_1$ (nm) ( $\pm 5$ nm)	$t_2$ (nm) ( $\pm 5$ nm)	$\epsilon_{\text{res}}(t_1)$ ( $\pm 1 \times 10^{-4}$ )	$\epsilon_{\text{res}}(t_2)$ ( $\pm 1 \times 10^{-4}$ )
S88	6.45	12.1	143	340	$0.44 \times 10^{-3}$	$3.11 \times 10^{-3}$
S89	6.8	12.3	239	244	$0.33 \times 10^{-3}$	$3.49 \times 10^{-3}$
S90	5.8	11.0	343	145	$0.92 \times 10^{-3}$	$4.16 \times 10^{-3}$
SS12	6.9	12.5	120	81	$4.18 \times 10^{-3}$	$8.12 \times 10^{-3}$
SS11	7.0	12.9	122	155	$3.5 \times 10^{-3}$	$6.40 \times 10^{-3}$
SS10	6.5	13	125	180	$1.32 \times 10^{-3}$	$4.72 \times 10^{-3}$
P-62 (step-graded)	$0.11 < x < 0.31$		1420			$3.7 \times 10^{-3}$
P-66 (lin. graded)	$0.12 < x < 0.29$		1020			$6.4 \times 10^{-3}$

from the Vegard's law and the RBS and HRXRD composition values.

## Results and Discussion

### Double layer heterostructures

The results of both RBS and HRXD measurements are reported in Table 1. The residual strain values versus the layer thickness of the structures investigated are shown in Figure 2. The points corresponding to the deeper ternary layers (filled circles) have been reported considering their individual thickness. The top layers show residual strain values much larger than predicted by the Matthews and Blakeslee model [22]. On the contrary, despite the lower In content, the deeper InGaAs buffer layers exhibit a much larger strain release and appear nearly completely relaxed. This simply evidences that the strain release of the first ternary layer depends on the total thickness of the structure that must be considered as a whole and not as made of two individual layers.

In all the samples, plan view room temperature SEM-PCL investigations in the transmission geometry revealed the presence of both the usual network of misfit dislocations (MDs) aligned in bands along the two  $\langle 110 \rangle$  type directions (Figs. 3a and 3b). Figures 3a and 3b represent two samples with dislocations only at the deeper interface and at both the interfaces respectively; this explains the difference in contrast sharpness between the two images. In Figure 3c, the corresponding plan view transmission electron micrograph of the sample of Figure 3b reveals the presence of curved dislocations (loops) and dislocations threading from the first to the second interface.

Further, plan view and XTEM investigations showed a much higher misfit dislocation density at the

Residual Parallel Strain vs thickness of the specimens investigated

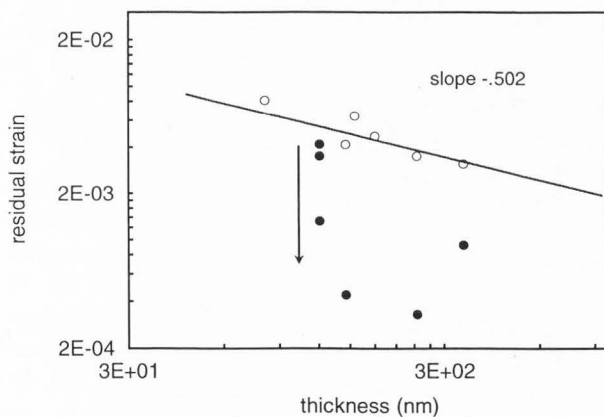


**Figure 2.** Residual strain versus specimen thickness. Continuous line: experimental curve obtained for InGaAs/GaAs single buffer layers [6]. Open circles correspond to external InGaAs layers; filled circles to the inner ternary layers. The vertical arrow shows the decrease of the residual strain by increasing the thickness of the uppermost layer in structures with constant thickness of the first InGaAs layer.

The residual parallel strain values,  $\epsilon^{\parallel}$ , were calculated from the composition values determined by RBS and HRXRD from the following equation:

$$\epsilon^{\parallel} = \left[ \frac{a^{\parallel} - a^0}{a^0} \right], \quad (2)$$

where  $a^0$  is the relaxed lattice parameter determined

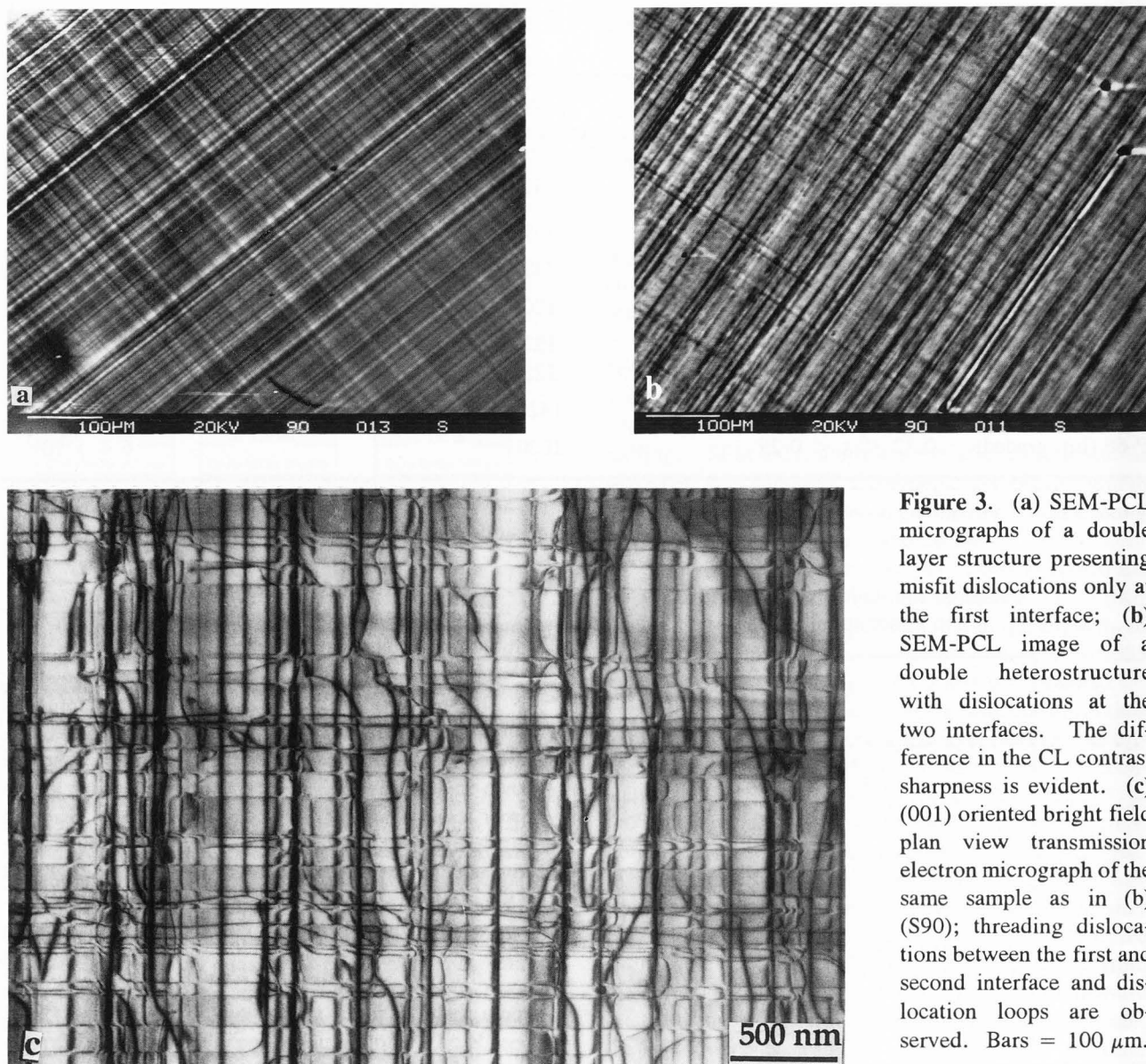


**Figure 3.** (a) SEM-PCL micrographs of a double layer structure presenting misfit dislocations only at the first interface; (b) SEM-PCL image of a double heterostructure with dislocations at the two interfaces. The difference in the CL contrast sharpness is evident. (c) (001) oriented bright field plan view transmission electron micrograph of the same sample as in (b) (S90); threading dislocations between the first and second interface and dislocation loops are observed. Bars = 100  $\mu\text{m}$ .

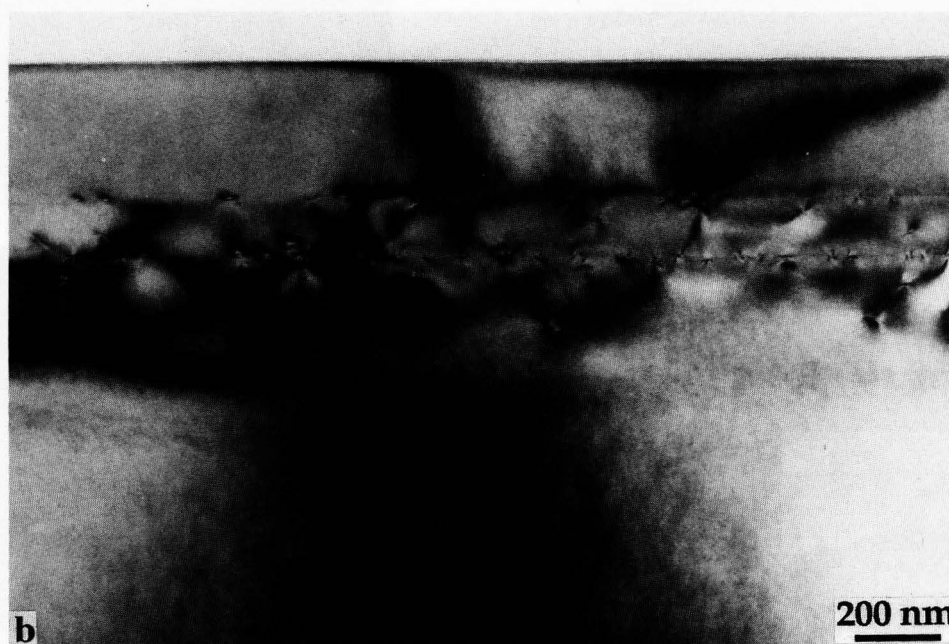
inner interface between the InGaAs layer and the substrate as shown, for example, in Figure 4 for the specimen S88. In the structure presenting the lower residual strain in the first ternary layer, the linear MD density at the InGaAs/GaAs interface was found to be at least 3-4 times higher than at the InGaAs/InGaAs one.

Besides misfit dislocations, both single and multiple dislocation loops extending mainly from the deeper interface inside the GaAs substrate were also found. Such a behaviour has been observed by other groups on SiGe/Ge [20] and InGaAs/GaAs [18] superlattices and graded heterostructures [3, 4, 16] and on InGaAs/GaAs single layers [8]. In SiGe/Si structures, the presence of these loops has been correlated to the activation of Frank-Read (F-R) sources for the generation of misfit dislocations

during the strain relaxation process. It is suggested that this kind of strain relaxation occurs only in very pure and slowly (1% misfit/ $\mu\text{m}$ ) compositionally-graded layers [20].

In all our samples, dislocation loops were found to propagate inside the substrate, even though the compositional gradient at the interface was practically infinite (step increase in composition). A similar finding was reported for InGaAs/GaAs single layers with  $x < 0.17$  by Krishnamoorthy *et al.* [16] who found dislocation loops in the GaAs substrate and no dislocations inside the layers. The results were interpreted on the basis of a balance of forces model and the introduction of a "critical composition difference" concept. Lefebvre *et al.* [18] also observed half-loops extending from the

**Figure 4.** (a) (001) oriented bright field plan view transmission electron micrograph of sample S88; the specimen has been thinned in the bevel geometry and the area with the lower dislocation density belongs to the external epilayer. (b) (110) oriented XTEM micrographs of the same structure as in (a) confirming the same ratio between the linear dislocation densities at the two interfaces.  $g = 004$  type.



interface inside the substrate in InGaAs/GaAs superlattices. The half-loops, acting as F-R dislocation sources, are the result of the glide of the inclined tip formed at the crossing point of two perpendicular dislocations. The glide toward the substrate is interpreted on the basis of misfit stress forces higher than the mutual interaction elastic forces.

The comparison of our results with the literature data suggests that an important parameter for confining dislocations far from the specimen surface in low mis-

matched heterostructures is the compositional gradient inside the layers. In case of structures with higher lattice mismatch, the starting compositional limit should be represented by the composition corresponding to transition from two-dimensional (2-D) to three-dimensional (3-D) nucleation [26]. In that case, the island coalescence mechanisms will rule the defect distribution inside the layer, and no defects will propagate inside the substrate as it is shown, for example, in [5].

XTEM maps obtained from several micrographs

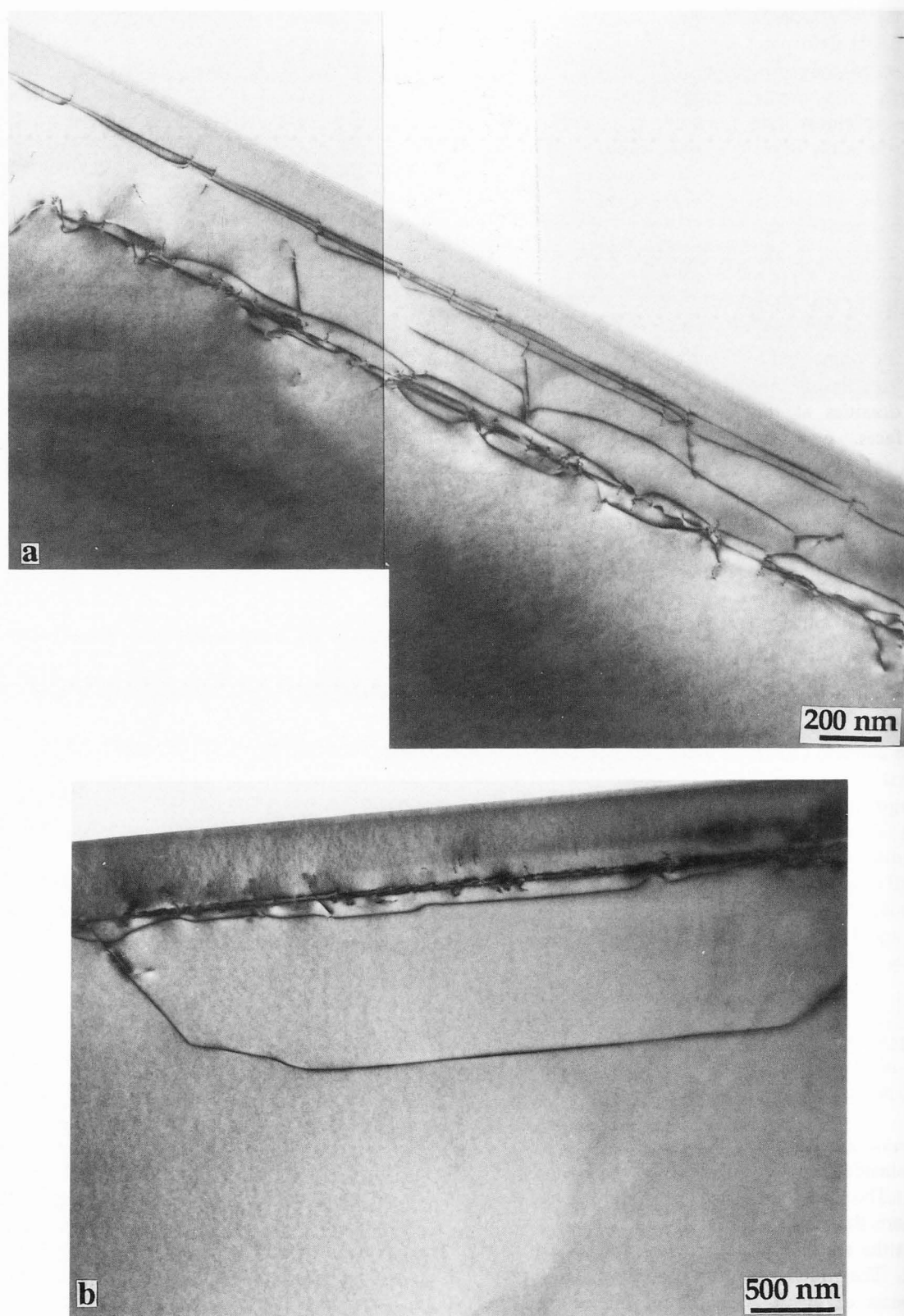


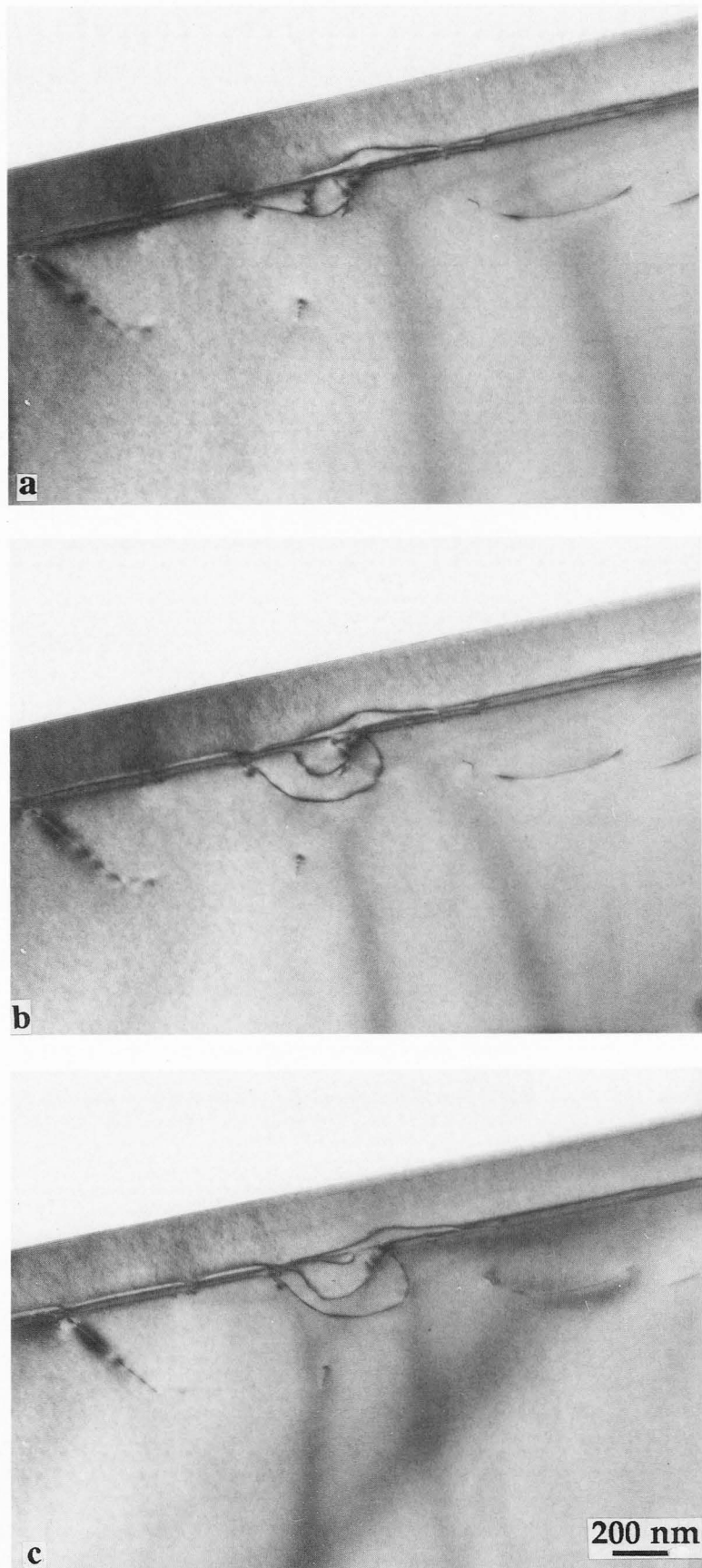
**Figure 5.** Bright field zone axis (110) oriented XTEM micrographs of (a) sample S90 and (b) sample S88. The dimension and penetration of dislocation loops inside the substrate is shown to increase by increasing the strain release in the inner layer.

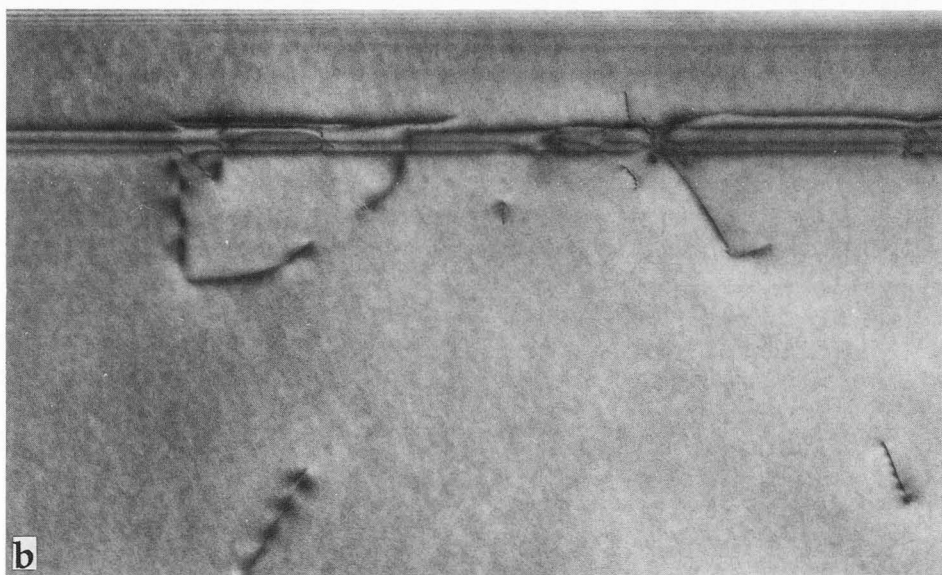
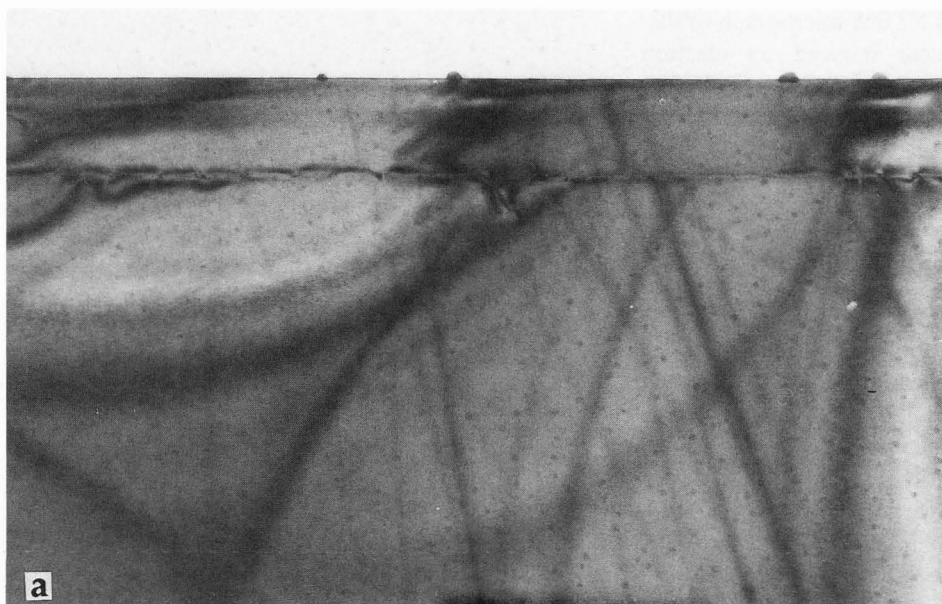
**Figure 6.** (110) XTEM micrograph of dislocation movement induced by electron beam irradiation in the TEM. (a) before irradiation, (b) and (c) during and after the dislocation movement.

showed that dislocation loops increased in dimension, density and penetration inside buffer layer and substrate by increasing the strain release inside the first InGaAs layer. Furthermore, threading dislocations start penetrating inside the first ternary layer up to the InGaAs/InGaAs interface as the residual strain of the inner layer decreases. Figure 5 shows, for comparison, two typical XTEM micrographs of the samples S90 (Fig. 5a) and S88 (Fig. 5b); the different dimension and penetration of the loops inside the GaAs buffer layer and substrate is apparent. Both misfit dislocations and dislocation loops were of  $60^\circ$  type with Burgers vector of  $a/2$  [110] type on a similar {111} glide plane.

The linear dislocation density required to accommodate the mismatch, as calculated by HRXRD measurements, is about  $2 \times 10^5 \text{ cm}^{-1}$  in the samples presenting the lower residual strain values. This value is higher than that one permitted by the number of available dislocations in the substrates. It follows that new dislocations must have been created either by a nucleation or multiplication process for releasing the strain. In these kinds of samples, F-R sources, which are a well documented way to generate dislocations [12, 23], can be provided by the pinning of dislocation segments due to dislocation intersections inside the MD network [13]. An example of one or more possible F-R sources is shown in Figure 6 where three loops are seen to slip and expand under the electron beam in the TEM. The slight inclination of the specimen (about  $10^\circ$ ) allows us to better observe the points of intersection of misfit dislocations on the interface plane that can lead to a F-R source.

The residual strain of the inner layer and the dislocation propagation from the first to the second interface have been studied as a function of the top layer thickness by investigating the structures SS10, SS11 and SS12 in Figure 1. Here, the inner





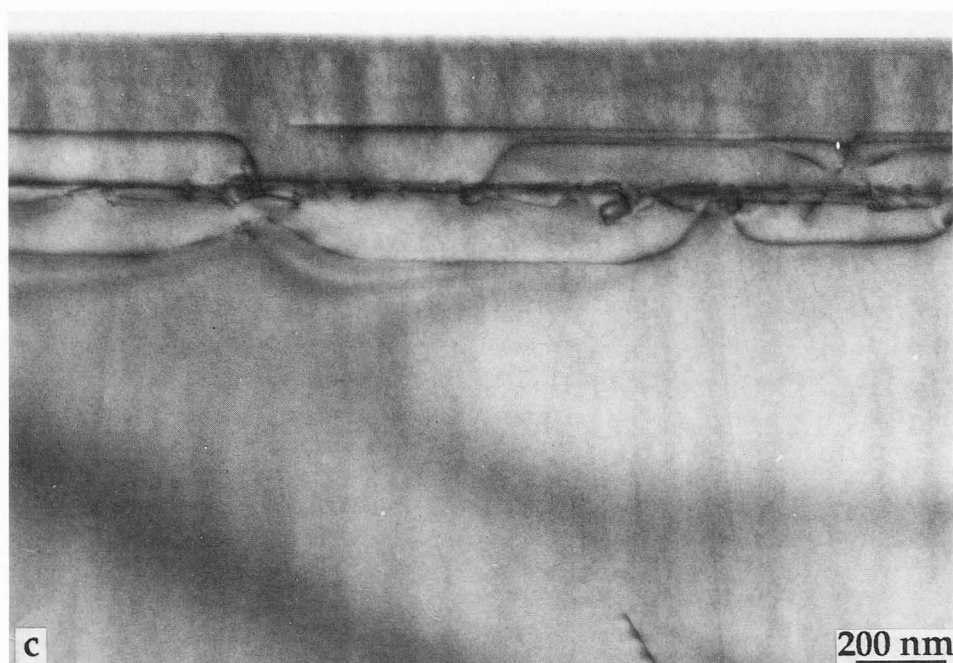
ternary layer is grown with constant thickness (120 nm) and composition ( $x = 0.05$ ), and the top one with variable thickness ( $80 < t_{ss} < 185$  nm) and constant composition ( $x = 0.10$ ). As pointed out by the vertical arrow in Figure 2, the residual strain of the three inner layers decreases by increasing the thickness of the uppermost layers and approaches the residual strain value of sample S88. A comparison of XTEM maps of the aforementioned samples (Fig. 7) shows that only a few single loops are revealed in the sample SS12, that multiple dislocation loops are present in sample SS11, and that the highest density of dislocation loops both inside the substrate and the inner epilayer is found in sample SS10

(Fig. 7c). This demonstrates that the dimension, location and penetration of multiple dislocation loops depend on the total amount of elastic energy in the structure and on the strain release in the inner InGaAs layer.

The residual parallel strain values of the upper layers are compared in Figure 2 with a unique curve of  $-1/2$  slope obtained from previous results on InGaAs/GaAs single heterostructures of similar composition and thickness [6] and in disagreement with the equilibrium theories [22]. This result leads to the assumption that, once the critical thickness is overcome, the elastic energy per unit interface area remains constant [24].

Our observations also reveal that dislocations first

**Figure 7.** Comparison between the (110) XTEM micrographs of the structures SS12 (a), SS11 (b) and SS10 (c). As expected, as the thickness of the external layer increases, dislocations start penetrating the first InGaAs layer and reach the second interface.



nucleate and multiply at the inner interface and that only when the dislocation density has reached the value corresponding to the minimum residual strain of the inner layer do the dislocations start crossing the first ternary layer. Also, the propagation of dislocation loops inside the substrate started only after all the dislocation sources in the substrate were almost exhausted.

From the XTEM micrographs, it can be noticed that no threading dislocations are visible in the external ternary layers. According to the typical specimen length and thickness investigated in the cross-section geometry, this corresponded to a maximum surface dislocation density of about  $6 \times 10^6 \text{ cm}^{-2}$ . The density of threading dislocations at the specimen surface was then measured by SEM-PCL investigations, DSL etching and plan view TEM maps on beveled samples. A maximum threading dislocation density of  $5 \times 10^5$  was evidenced in the most defective double heterostructures (SS10). This result can be interpreted on the basis of the operation of pinning mechanisms of threading dislocations by intersecting misfit dislocations [11, 14].

### Graded heterostructures

A similar study was performed on MBE grown InGaAs/GaAs linearly-graded and step-graded buffer structures. Figure 8a shows a XTEM micrograph of a linear-graded InGaAs/GaAs sample of nominal composition  $0.1 < x < 0.3$  and thickness  $t_{lg} = 1.02 \mu\text{m}$ . The majority of dislocations are distributed across about the first 600 nm of the layer thickness, leaving a consistent portion of the structure almost free of defects. The

threading dislocation density was estimated to be about  $4\text{-}5 \times 10^5 \text{ cm}^{-2}$ . Similar to the double layer structures, the highest dislocation density is at the interface between substrate and graded layer and some loops are present in the GaAs substrate. After the first critical thickness is overcome, MDs most likely nucleate from pre-existing substrate dislocations at the interface and start releasing the strain. As the growth continues, the number of dislocations at the interface increases until the initial misfit is released. At this time during the growth, there is still elastic energy inside the structure and more dislocations are needed to release the excess of elastic energy. Once a new critical thickness is overcome, new dislocations nucleate, for example, as a consequence of heterogeneous nucleation or from some threading segments coming from the inner portion of the layer, and propagate from the growth surface toward the interface. A residual strain of the order of magnitude of  $2 \times 10^{-4}$  still remains at the interface. It follows that dislocations can propagate at a distance that depends on the misfit gradient inside the structure and, in particular, the distance from the misfit gradient at the moment of the plastic release. A minimum distance from the preexisting dislocations of about 18 nm can be calculated by:  $\epsilon = \Delta f t_s = (f/t_{lg}) t_s$ , where  $\epsilon$  is the residual strain at the interface,  $\Delta f$  is the misfit gradient,  $f$  is the misfit,  $t_{lg}$  is the thickness of the linear-graded layer and  $t_s$  is the distance at which the new dislocations stop with respect to the previous ones. Therefore, dislocations almost regularly distributed inside the layer, in a similar way of a step-graded structure, should be expected. This is confirmed by the XTEM micrograph (Fig. 8a). It is worth noting

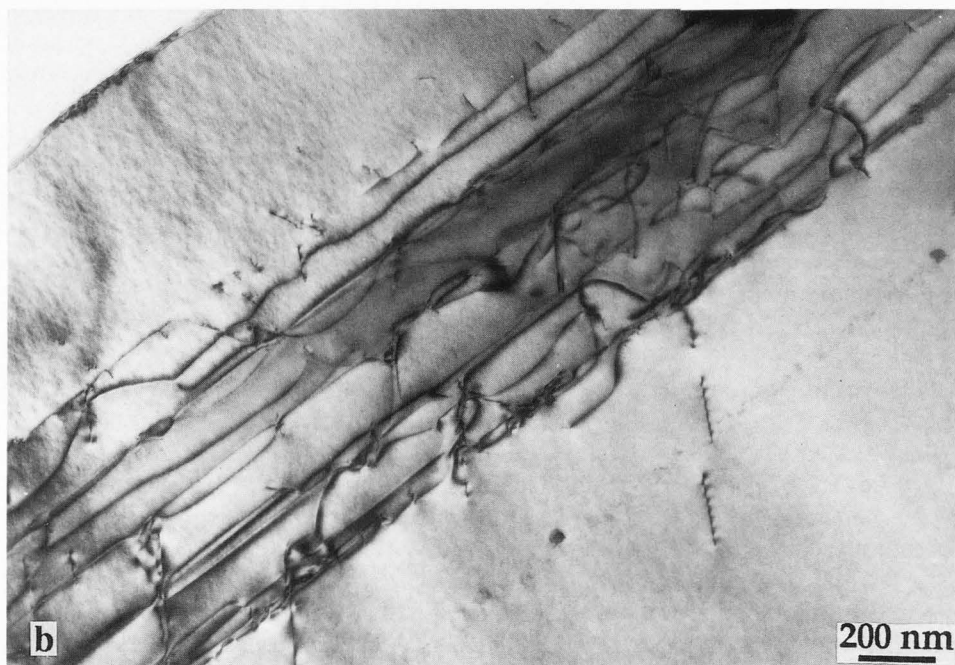
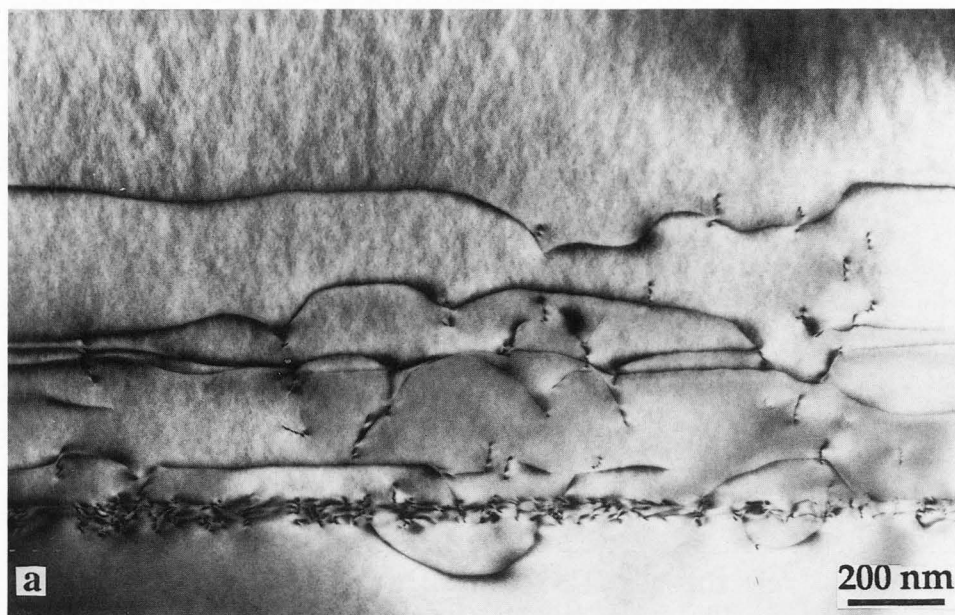


**Figure 8.** (a) (110) oriented bright field zone axis XTEM micrograph of the linear-graded heterostructure. Dislocation uniformly distributed inside the layer are shown. (b) Step-graded structure. Dislocations propagating from the deeper interface through the structure are shown. Dislocation pile-up is also present in the substrate. The highest MD density is at the InGaAs/GaAs interface for both the samples; furthermore, the two layers present a portion of some hundreds nanometer thick free of defects in the limit of the cross-sectional TEM analyses.

that secondary ion mass spectrometry (SIMS) analyses did not show any step-like behaviour of the composition inside the layer. Since the higher the misfit gradient is, the lower the distance is between dislocations generated at different moments during the growth, the slope of the misfit curve is also important for the dislocation distribution inside a linear-graded structure.

A step-graded layer with nominal composition,  $0.1 < x < 0.3$  and  $t_{sg} = 1.02 \mu\text{m}$  and a cap layer of nomi-

nal composition  $x = 0.3$  and thickness of 400 nm for simulating a complete buffer for device applications was also studied by XTEM investigations (Fig. 8b). In this case also, in agreement with the findings on double and linear-graded heterostructures, the highest misfit dislocation density was found at the first heterointerface. In this case, in contrast to the linear-graded layer, dislocation pile-up was found in the GaAs substrate at a depth of  $\sim 0.5 \mu\text{m}$ . Additional misfit dislocations were

distributed throughout the layers with different In concentration and were mainly positioned at each interface. Further, their density decreased by increasing the In concentration, leaving the additional top layer with  $x = 0.3$  with a dislocation density of about  $6 \times 10^5 \text{ cm}^{-2}$ . This shows the reliability of the structures as buffer layers for reducing the dislocation density at the specimen surface as already found by other groups [2, 4].

The observation of dislocations pile-up together with the results on the linear-graded specimen confirm that the compositional step and the strain gradient must be considered as a whole in low lattice mismatched buffer layers. Therefore, in a step-graded structure, it follows that the number of layers necessary to design prefixed surface lattice parameter and residual strain values is related to the maximum composition step between successive layers, the maximum composition step being determined by the 2D-3D growth transition regime. Work is in progress for developing a numerical model to account for strain release in multiple structures.

#### Lattice planes tilting in double heterostructures

According to the works of Ayers *et al.* [1] and of Kavanagh *et al.* [15], HRXRD investigations showed small tilts (300-400 sec. of arc) between the buffer layer lattice and the substrate lattice in all the samples. These tilt angles, observed by HRXRD after a  $180^\circ$  rotation along the sample surface axis with the same diffraction geometry, were due to the low angle grain boundary produced by the dislocation network at the buffer layer-substrate interface. Moreover, this tilting effect did not appear to be correlated with the asymmetry of the strain release found in several samples along the two (110) directions parallel to the interface. The tilt value  $\alpha$  is related to the imbalance,  $(\rho^+ - \rho^-)$ , in the linear density of dislocations having opposite  $b \perp^{\text{eff}}$  component of the Burgers vector perpendicular to the interface [23]:

$$\alpha = b \perp^{\text{eff}} (\rho^+ - \rho^-) \quad (3)$$

Assuming that only  $60^\circ$  dislocations with  $b \perp = a/2$  are present, the tilt of 400 seconds of an arc observed in the sample S88 corresponds to a linear dislocation density  $(\rho^+ - \rho^-) = 6.86 \times 10^4 \text{ cm}^{-1}$ . The comparison with the dislocation density determined by TEM and HRXRD,  $1.14 \times 10^5 \text{ cm}^{-1}$  indicates that the majority of the dislocations have the same perpendicular component of the Burgers vector. A similar result obtained by Kavanagh *et al.* [15] in InGaAs/GaAs samples cut  $2^\circ$  off the (100) planes could be interpreted as due to a preferential generation of dislocations having the same perpendicular component of the Burgers vector determined by the different degree of strain release associated to opposite

components  $b \perp$ . In the present case, the very low surface miscut angle cannot explain such difference. In most samples, the surface miscut was measured by HRXRD by comparing the Bragg angle position after  $180^\circ$  rotation. The maximum miscut angle found was  $0.2^\circ$  with no correlation between the layer lattice tilt and the miscut direction. Since the low dislocation density for the Si doped GaAs substrate (about  $5.5 \times 10^2 \text{ cm}^{-2}$ ) can accommodate only a small part of the strain according to the Matthews model, we conclude that the dislocation multiplication mechanism is responsible for such difference and that mainly dislocations of the same type are generated.

#### Conclusions

Double InGaAs/GaAs heterostructure buffer layers were revealed to be effective in confining MDs at the deeper interface. The strain release behaviour has been explained on the basis of previous results on single InGaAs/GaAs layers, showing that the elastic energy per unit interface area remains constant. The strain relaxation occurs through dislocation multiplication due to Frank-Read source activated during the growth, as shown by numerous dislocation loops inside the substrate. Lattice plane tilts between epilayers and substrates of the order of magnitude of some hundred seconds of arc have been found. The tilt is determined by the imbalance in the linear density of misfit dislocations with opposite  $b \perp^{\text{eff}}$  component of the Burgers vector perpendicular to the interface. The possibility of growing buffer layers with prefixed residual strain and composition has been shown to be related to the maximum concentration step between successive layers for step-graded heterostructures and to the misfit gradient inside the layer for linear-graded structures.

#### Acknowledgements

Thanks are due to Dr. F. Genova from CSELT for growing the graded heterostructures. Special thanks are due to Dr. Jan Weyher for DSL chemical etching assistance.

#### References

- [1] Ayers JE, Ghandhi SK, Schowalter LJ (1991). Crystallographic tilting of epitaxial layers. *J. Cryst. Growth* **113**: 430-440.
- [2] Chang JCP, Chen J, Fernandez JM, Wieder HH, Kavanagh KL (1992). Strain relaxation of compositionally graded  $\text{In}_x\text{Ga}_{1-x}\text{As}$  buffer layers for modulation-doped  $\text{In}_{0.3}\text{Ga}_{0.7}\text{As}/\text{In}_{0.29}\text{Al}_{0.71}\text{As}$  heterostructures. *Appl. Phys. Lett.* **60**: 1129-1131.

- [3] Chang JCP, Chin TP, Tu CW, Kavanagh KL (1993). Multiple dislocation loops in linear-graded  $\text{In}_x\text{Ga}_{1-x}\text{As}$  ( $0 \leq x \leq 0.53$ ) on GaAs and  $\text{In}_x\text{Ga}_{1-x}\text{P}$  ( $0 \leq x \leq 0.32$ ) on GaP. *Appl. Phys. Lett.* **63**: 500-502.
- [4] Chang KH, Bhattacharya PK, Lai R (1990). Lattice mismatched  $\text{In}_{0.53}\text{Ga}_{0.47}\text{Al}_{0.48}\text{As}$  modulation-doped field-effect transistors on GaAs: molecular beam epitaxial growth and device performance. *J. Appl. Phys.* **67**: 3323-3327.
- [5] Chang S, Chang T, Lee S (1993). The growth of highly mismatched  $\text{In}_x\text{Ga}_{1-x}\text{As}$  ( $0.28 < x < 1$ ) on GaAs by molecular-beam-epitaxy. *J. Appl. Phys.* **73**: 4916-4926.
- [6] Drigo AV, Aydinly A, Camera A, Genova F, Rigo C, Ferrari C, Franzosi P, Salviati G (1989). On the mechanisms of strain release in molecular-beam-epitaxy-grown  $\text{In}_x\text{Ga}_{1-x}\text{As}/\text{GaAs}$  single heterostructures. *J. Appl. Phys.* **66**: 1975-1983.
- [7] Drigo AV, Mazzer M, Romanato F (1992). Ion beam analysis of mismatched epitaxial heterostructures. *Nucl. Instr. and Methods B***63**: 30-35.
- [8] Fitzgerald EA, Ast DG, Kirchner PD, Pettit GD, Woodall JM (1988). Structure and recombination in  $\text{InGaAs}/\text{GaAs}$  heterostructures. *J. Appl. Phys.* **63**: 693-703.
- [9] Fitzgerald EA, Xie YH, Breen ML, Brasen D, Kortan AR, Michel J, Mii YJ, Weir BE (1991). Totally relaxed  $\text{Ge}_x\text{Si}_{1-x}$  layers with low threading dislocation densities grown on Si substrates. *Appl. Phys. Lett.* **59**: 811-813.
- [10] Fitzgerald EA, Xie YH, Monroe D, Silverman PJ, Kuo JM, Kortan AR, Thiel FA, Weir BE (1992). Relaxed  $\text{Ge}_x\text{Si}_{1-x}$  structures for III-V integration with Si and high mobility two-dimensional electron gases in Si. *J. Vac. Sci. Technol.* **B10**: 1807-1819.
- [11] Freund LB (1990). A criterion for arrest of a threading dislocation in a strained epitaxial layer due to an interface misfit dislocation in its path. *J. Appl. Phys.* **68**: 2073-2080.
- [12] Herbeaux C, DiPersio J, Lefebvre A (1989). Misfit dislocations in  $\text{In}_{0.15}\text{Ga}_{0.85}\text{As}/\text{GaAs}$  strained layer superlattices. *Appl. Phys. Lett.* **54**: 1004-1006.
- [13] Hirte JP, Lothe J (1982). *Theory of Dislocations*. 2nd ed. Wiley, NY. chap. 20, 751-754.
- [14] Hull R, Bean JC, Buescher C (1989). A phenomenological description of strain relaxation in  $\text{Ge}_x\text{Si}_{1-x}/\text{Si}$  (100) heterostructures. *J. Appl. Phys.* **66**: 5837-5843.
- [15] Kavanagh KL, Chang JCP, Chen J, Fernandez JM, Wieder HH (1992). Lattice tilt and dislocations in compositionally step-graded buffer layers for mismatched  $\text{InGaAs}/\text{GaAs}$  heterointerfaces. *J. Vac. Sci. Technol.* **B10**: 1820-1823.
- [16] Krishnamoorthy V, Ribas P, Park RM (1991). Strain relief study concerning the  $\text{In}_x\text{Ga}_{1-x}\text{As}/\text{GaAs}$  ( $0.07 < x < 0.5$ ) material system. *Appl. Phys. Lett.* **58**: 2000-2002.
- [17] Krishnamoorthy V, Lin YW, Park RM (1992). Application of "critical compositional difference" concept to the growth of low dislocation density ( $< 10^4/\text{cm}^2$ )  $\text{In}_x\text{Ga}_{1-x}\text{As}$  ( $x < 0.5$ ) on GaAs. *J. Appl. Phys.* **72**: 1752-1757.
- [18] Lefebvre A, Herbeaux C, DiPersio J (1991). Interactions of misfit dislocations in  $\text{In}_x\text{Ga}_{1-x}\text{As}/\text{GaAs}$  interfaces. *Phil. Mag. A* **63**: 471-485.
- [19] LeGoues FK, Meyerson BS, Morar JF (1991). Anomalous strain relaxation in SiGe thin films and superlattices. *Phys. Rev. Lett.* **66**: 2903-2906.
- [20] LeGoues FK, Meyerson BS, Morar JF, Kirkner PD (1992). Mechanisms and conditions for anomalous strain relaxation in graded thin films and superlattices. *J. Appl. Phys.* **71**: 4230-4243.
- [21] Lord SM, Pezeshki B, Kim SD, Harris SJ Jr (1993).  $1.3 \mu\text{m}$  Exciton resonances in  $\text{InGaAs}$  quantum wells grown by molecular beam epitaxy using a slowly graded buffer layer. *J. Cryst. Growth* **127**: 759-764.
- [22] Matthews JW, Blakeslee AE (1974). Defects in epitaxial multilayers. I. Misfit dislocations. *J. Cryst. Growth* **27**: 118-125.
- [23] Mazzer M, Camera A, Drigo AV, Ferrari C (1990). Elastic distortion field in single layer heterostructures in the presence of misfit dislocations. *J. Appl. Phys.* **68**: 531-539.
- [24] Romanato F (1994). Study and structural characterization of compound semiconductors epitaxial layers. Ph.D. Thesis. Physics Department, University of Padova, Italy. Ch. 6, 4-12.
- [25] Salviati G, Ferrari C, Lazzarini L, Nasi L, Norman CE, Bruni MR, Simeone MG, Martelli F (1993). Electron microscopy and X-ray diffraction determinations of strain release in  $\text{InGaAs}/\text{GaAs}$  superlattices grown by molecular beam epitaxy. *J. Electrochem. Soc.* **140**: 2422-2427.
- [26] Tersoff J, LeGoues FK (1994). Competing relaxation mechanisms in strained layers. *Phys. Rev. Lett.* **72**, 3570-3573.

#### Discussion with Reviewers

**L. Schowalter:** While it may be possible that a particular defect would tend to punch out MDs which have the same Burgers vector, without some symmetry breaking mechanism, the average tilt of a large enough area would still have to be zero. How big an area do the authors measure? For different samples, is the tilt always in the same azimuthal direction?

**Authors:** In the majority of the samples we investi-

gated, area corresponded to the X-ray beam size, that is  $\sim 1 \text{ mm}^2$ . In a few samples, the uniformity was verified. Peak shifts lower than a few % were found in areas of  $1 \text{ cm}^2$  in size. Different amounts of tilt were found along the two  $\langle 110 \rangle$  directions in the samples without any correlation to the strain release.

**F. LeGoues:** I think that the data presented are completely consistent with those of Kavanagh *et al.* [15], Mooney *et al.* (1994) and LeGoues *et al.* (1993). In all of these, the tilt depends on the mismatch, the growth temperature and the initial miscut. Without treating all of these, and comparing with previous theories, the authors cannot state that "the miscut angle cannot explain such difference." Indeed, a small tilt such as observed here is completely consistent with the values found by Kavanagh, Legoue for a miscut of  $0.5^\circ$ . Furthermore, the multiplication mechanism cannot explain the tilt by itself. As shown by LeGoues *et al.*, the miscut results in the reproduction of only one set of dislocations. Without the miscut, it is impossible to figure out why one set would reproduce preferentially.

**Authors:** We do not state that the tilt angle is independent of the surface miscut for any value of the miscut angle. We simply say that, in the present case, with miscut angles lower than  $0.5^\circ$  ( $0.2^\circ$  in the samples tested), the tilt is not determined by the miscut. In fact, for miscut angles of  $0.2^\circ$ , the increase of the edge component of the Burgers' vector of a MD is only  $2.5 \times 10^{-3}$  which does not seem to be sufficient to explain the broken symmetry. The existing TDs type in the substrates could be a possible reason for that.

#### Additional References

Mooney PM, LeGoues FK, Tersoff J, Chu JO (1994). Nucleation of dislocations in SiGe layers grown on (001) Si. *J. Appl. Phys.* **75**: 3968-3977.

LeGoues FK, Mooney PM, Tersoff J (1993). Measurement of the activation barrier to nucleation of dislocations in thin films. *Phys. Rev. Lett.* **71**: 396-399.